Environmental Science & Technology

pubs.acs.org/est

Article

High-Spatial-Resolution Estimates of Ultrafine Particle Concentrations across the Continental United States

Provat K. Saha, Steve Hankey, Julian D. Marshall, Allen L. Robinson,* and Albert A. Presto*

Cite This: *Environ. Sci. Technol.* 2021, 55, 10320−10331

Read Online

ACCESS | Metrics & More | Article Recommendations | Supporting Information

ABSTRACT: There is growing evidence that ultrafine particles (UFP; particles smaller than 100 nm) are likely more toxic than larger particles. However, the health effects of UFP remain uncertain due in part to the lack of large-scale population-based exposure assessment. We develop a national-scale empirical model of particle number concentration (PNC; a measure of UFP) using data from mobile monitoring and fixed sites across the United States and a land-use regression (LUR) modeling framework. Traffic, commercial land use, and urbanicity-related variables explain much of the spatial variability of PNC (base model R^2 = 0.77, RMSE = 2400 cm^{-3}). Model predictions are robust across a diverse set of evaluations [random 10-fold holdout cross-validation (HCV): R^2 = 0.72, RMSE = 2700 cm^{-3}; spatially defined HCV: R^2 = 0.66, RMSE = 3000 cm^{-3}; evaluation against an independent data set: R^2 = 0.54, RMSE = 2600 cm^{-3}]. We apply our model to predict PNC at ∼6 million residential census blocks in the contiguous United States. Our estimates are annual average concentrations for 2016−2017. The predicted national census-block-level mean PNC ranges between 1800 and 26 600 cm^{-3} (population-weighted average: 6500 cm^{-3}), with hotspots in cities and near highways. Our national PNC model predicts large urban−rural, intra-, and inter-city contrasts. PNC and $PM_{2.5}$ are moderately correlated at the city scale, but uncorrelated at the regional/national scale. Our high-spatial-resolution national PNC estimates are useful for analyzing population exposure (socioeconomic disparity, epidemiological health impact) and environmental policy and regulation.

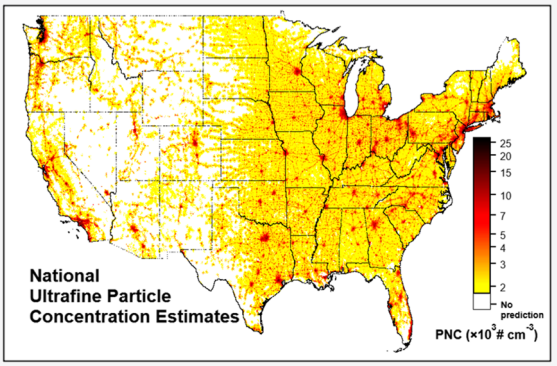

KEYWORDS: *ultrafine particles, spatial modeling, exposure assessment*

1. INTRODUCTION

The health effects of fine particulate matter mass ($PM_{2.5}$) are well established.[1] However, uncertainty remains about what characteristics of $PM_{2.5}$, such as sources, composition, and size, are most responsible for the observed health effects.[2,3] Some researchers have proposed that ultrafine particles (UFP; particles smaller than 100 nm) have higher toxicity than larger particles. There is some toxicological evidence to support this hypothesis.[4−9] Some city-scale epidemiology studies also suggest possible UFP health effects, but outcomes are inconsistent and inconclusive between different studies.[2,10−12] A recent systematic review found evidence for adverse short-term associations between UFP and inflammatory and cardiovascular changes that may be at least partly independent of other pollutants.[13] However, the evidence for independent, chronic health effects of UFP remains inconclusive or insufficient.[2,13]

A major obstacle for UFP epidemiological studies is the lack of long-term, large-spatial-scale exposure estimates.[2,13−15] This is due to a number of factors. First, exposure assessment for UFP is hindered by the lack of routine monitoring networks. Therefore, existing UFP epidemiological studies rely on short-term data collection in specific cities,[10,11] which lack the potentially larger urban−rural and intercity contrasts that national estimates may provide. Second, UFP concentrations are highly spatially variable within cities.[3,14,16−20] Therefore, the spatial patterns of UFP will not be resolved using a traditional national monitoring strategy of a small number (1−5) of sites per city, usually located to capture "urban background" locations.[21−23] That approach is reasonable for $PM_{2.5}$ since intraurban differences are modest, but is unlikely to capture the variability in UFP concentrations.[16,22,24] UFP characterization needs data on both intra- and interurban variations.[6,25] Third, previous research indicates some spatial correlation of $PM_{2.5}$ mass and UFP (R^2 ∼ 0.4) at the urban scale,[26−28] which may complicate differentiating their independent health effects.

One way to overcome some of these challenges is through national-scale UFP concentration estimates at a high spatial

Received: May 19, 2021
Revised: July 2, 2021
Accepted: July 9, 2021
Published: July 21, 2021

https://doi.org/10.1021/acs.est.1c03237
Environ. Sci. Technol. 2021, 55, 10320−10331

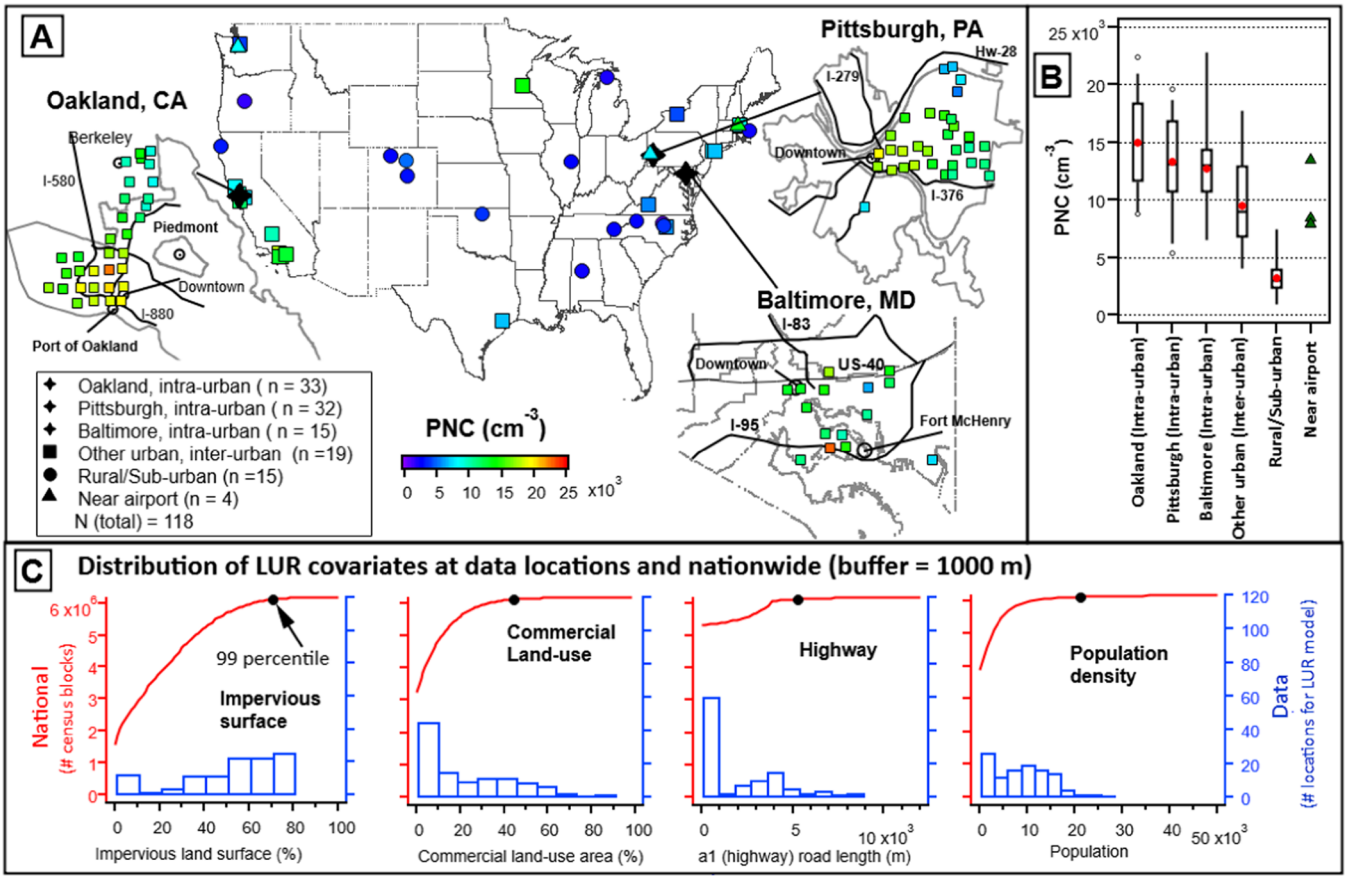

Figure 1. Data set used for LUR model development. (A) Measurement locations are colored by the average PNC at each site. Inset city maps show the high-spatial-resolution mobile monitoring data from Oakland, Pittsburgh, and Baltimore. (B) Distribution of PNC at fixed sites and 1 km^2 grid average PNC measured with mobile monitoring in three target cities. The box shows the interquartile range; the line inside the box is the median; whiskers indicate 5th and 95th percentiles, small gray circles show individual outliers, and the red circle represents the mean. (C) Distribution of major land-use covariates at UFP measurement locations (118 points shown in A) and nationwide census blocks (n = 6 174 588). Histograms (blue) show the distribution of covariates across measurement locations in 10 equally spaced bins. Cumulative frequency distribution (CDF; red curve) shows the national census block distribution. The black circle on the red curve is the 99th percentile value of the national distribution. Figure S6 in the Supporting Information (SI) is the extended version of panel (C). It shows the distribution of various land-use covariates for 500 and 1000 m buffer sizes. The a1 type road is a primary road with limited access or interstate highway.

resolution that capture intracity variation, interurban variation, and urban−rural gradients. We develop a national model for ambient UFP concentrations in the United States (US). Our novel approach combines (1) highly spatially resolved mobile measurements in three US cities to capture intraurban variations, (2) longer-term fixed-site data from various urban locations across the United States to characterize interurban trends, and (3) longer-term data from rural locations to capture urban−rural gradients. We apply an empirical modeling approach [also known as land-use regression (LUR)] to these data to develop the first national-scale estimates of outdoor UFP concentrations for census blocks across the contiguous United States. We discuss the implications of our results for epidemiology, environmental policy, and regulations in the United States.

2. MATERIALS AND METHODS

2.1. Ultrafine Particle Data Set. We use total particle number concentration (PNC) as a measure of UFP.[17] To develop our empirical model, we analyzed a national PNC data set (Figure 1 and Table S1) that consists of longer-term fixed-site measurements from (i) 19 urban locations in 19 cities, (ii) 15 rural locations, and (iii) 4 near airport locations as well as (iv) spatially dense intraurban mobile monitoring data from three cities (Pittsburgh PA, Oakland CA, Baltimore, MD). We compiled fixed-site data from the literature. Mobile monitoring data are discussed in Presto et al.[29] We briefly describe each component below.

To characterize background levels, we compiled PNC measurements from 15 rural locations across the United States (Table S1). We obtained these data from the NOAA Earth System Research Laboratories webpage (https://www.esrl.noaa.gov/gmd/aero/net/stations.html) [Southern Great Plains (SGP), OK; Bondville, IL; Steamboat Springs, CO; Mt. Bachelor, OR; Cape Cod, MA; Trinidad Head, CA; Boone, NC; Table Mt, CO], and other field campaigns (Centreville, AL; Manitou Forest, CO; UMBS, MI; Duke Forest, NC; Look Rock, TN; Durham, NC; Fox Chapel, PA).

To characterize interurban variability, we compiled PNC measurements from 19 urban fixed sites in 19 cities (Table S1): Queens NY, Long Island NY, Rochester NY, Boston MA, Somerville MA, Minneapolis MN, Raleigh NC, Houston TX, Blacksburg VA, Seattle WA, and nine cities in California (Livermore, Redwood, San Pablo, Santa Rosa, Los Angeles, Anaheim, Compton, Rubidoux, and Bakersfield).

https://doi.org/10.1021/acs.est.1c03237
Environ. Sci. Technol. 2021, 55, 10320−10331

The influence of airports on local UFP concentrations has been reported in several studies.[30−32] We compiled PNC measurements from four near airport fixed sites located within 5 km from the airport (Table S1): Logan International Airport, Boston, MA, Pittsburgh International Airport, Pittsburgh, PA, and Seattle-Tacoma International Airport, Seattle, WA (two sites).

To complement the fixed-site data, and to characterize the intraurban spatial variability of PNC, we performed targeted mobile sampling in three cities. Specifically, we carried out saturation sampling (driving on every street on every day) in multiple neighborhoods in each city and on multiple days in each city: Oakland (20 days; 2017), Pittsburgh (13 days; 2019), and Baltimore (10 days; 2019).

2.2. Data Reduction and Quality Assurance of Ultrafine Particle Data. Data reduction and quality assurance methods for mobile sampling data are described in Saha et al.[16] and Presto et al.[29] The same instrumentation [a condensation particle counter (CPC),[33] lower size cut of 5 nm] and sampling approach were used in all three cities. We averaged raw mobile monitoring measurements over space and time to determine stable mean concentrations on a 1 km^2 grid, following the approach of Shah et al.[22,34,35] Briefly, we first calculated the median concentration measured in each 1 km^2 grid cell on each sampling day, and then the mean of medians across all sampling days. Recent mobile sampling research[36−38] suggests that between 7 and 15 days of repeated sampling are needed to characterize a representative stable mean concentration for PNC LUR modeling in the absence of true long-term average measurements. Therefore, we only used grid cells with 7 or more days of measurements (range 7−20 days) in the modeling analysis. This inclusion criterion yielded PNC data for 33 1 km^2 grid cells in Oakland, 32 in Pittsburgh, and 15 in Baltimore.

We used a 1 km^2 grid to aggregate the mobile monitoring data because the resulting number of data points avoids overweighting urban sites in the regression analysis. Since we have only 15 rural sites, adding too many urban points biases the regression toward urban locations. The resulting number of mobile monitoring data points in each city (20−40) using a 1 km^2 grid averaging is comparable to that of previous city-level exposure studies (e.g., ESCAPE study).[39,40]

To investigate the influence of grid resolution on our results, we performed a sensitivity analysis using mobile monitoring data compiled on a 200 × 200 m^2 grid.[29] Figure S1 shows the comparison of 200 × 200 m^2 versus 1 km^2 data; the 5th and 95th percentiles range of concentration distributions from different cities agreed within 2−13%. For sensitivity analysis, we randomly divided 200 × 200 m^2 grid data from each city (Oakland: 373, Pittsburgh: 219, Baltimore: 108) into nine subsets and developed nine models using each subset from each city, along with other fixed-site data.

Table S1 lists the collection year and temporal coverage for fixed-site data. All of these measurements were collected using a condensation particle counter (CPC) or scanning mobility particle sizer (SMPS) system; the lower size cut is ∼5−10 nm in most cases (Table S1). About 60% of fixed sites (22 out of 38) have at least 1 year of data, and only four sites have 1 month of data (the minimum criteria for inclusion in the data set). We computed the annual average (or the average of all available data) from each site for model building.

Our LUR model predicted annual average outdoor UFP concentrations in 2016−2017. Therefore, if available, we used data from 2016 to 2017 for model development (33% of the fixed-site data are from that year). However, if not available, we used data from other years as well, but not older than 2009. For data not collected in 2016−2017 and/or collected for only part of the year, we applied two temporal correction factors: (i) annual factor and (ii) seasonal factor. The annual factors are applied to the data collected in a year other than 2016−2017. The seasonal factors are applied to data that do not have coverage throughout a full year.

Annual correction factors were applied to data from 25 fixed sites and mobile data from Pittsburgh (2019) and Baltimore (2019). We derived annual correction factors by fitting long-term (2006−2016) annual average PNC concentrations measured at four sites as a function of years (Rural: SGP, OK; Bondville, IL; Urban: Rochester NY; and Boston MA) (Figure S2). The fit indicates a 2% decrease in annual average concentrations per year. The correction factors vary by year, ranging between 0.89 and 1.06 (for, 2016−2017, AF = 1; before 2016, AF < 1; after 2017, AF > 1).

Seasonal factors are applied to data from 14 fixed sites and mobile sampling data from three cities. We derived seasonal correction factors by fitting the ratios of monthly-to-annual-average measured PNC data from 10 sites (seven urban and three rural sites) (Figure S3). We used the average of ratios from three consecutive years (2014−2016) to get a stable profile. The seasonal correction factors varied from 0.94 and 1.09, with higher PNC in the winter than in the summer months.

Annual and seasonal correction factors are small compared to a factor of 20 spatial variations in measured PNC (Figure 1B).

We also evaluated a number of other factors that may influence the robustness of PNC data set, including: (i) differences in instrumental size cut, (ii) mobile versus stationary sampling, and (iii) impact of new particle formation (nucleation) events. Overall, the uncertainty associated with each of these factors is relatively small (roughly within ±15%) (see Figures S4 and S5) compared to the factor of 20 spatial variations in measured PNC (∼1000−20 000 cm^{-3}, Figure 1). Furthermore, each of these issues likely impacts only a small fraction of data. Each of these factors is briefly discussed below.

One potential concern is differences in instrument size cut. Mobile monitoring was performed using the same CPC with a 5 nm lower size cut; therefore, differences in instrumental size cut is not an issue for this data set. However, it is a concern for the fixed-site data, which used different instruments with size cuts ranging from 4 to 20 nm (Table S1). Figure S4 shows size distribution data from three sites: a rural background (Look Rock, TN), an urban background (Carnegie Mellon University, Pittsburgh, PA), and a city center (Downtown, Pittsburgh, PA). The fractions of total long-term average PNC below 20 nm at these sites are 3, 11, and 44%, respectively. This suggests that long-term average PNC measured at rural and urban background locations are not strongly influenced by differences in instrument size cut (biases less than 11%). However, differences in size cut can be more significant in downtown locations (up to almost a factor of 2). Fortunately, all of the urban core PNC data used in our analysis is from mobile monitoring, which used the same instrument with a 5 nm size cut. Therefore, our urban core data should not be systematically biased. Finally, even a worst-case scenario of a factor of 2 bias in downtown locations is still much smaller than the measured PNC variability (Figure 1B). No

https://doi.org/10.1021/acs.est.1c03237
Environ. Sci. Technol. 2021, 55, 10320−10331

corrections were made to the data for differences in instrument size cut.

Another potential concern is systematic biases between mobile and fixed-site sampling. A comparison of our Pittsburgh mobile data with an independent PNC data set from 30 fixed locations in Pittsburgh[16] does not show any systematic biases between mobile and fixed-site data (Figure S5). Previous studies that have reported differences only considered short-term data collected over a limited number of repeated days.[41,42]

Finally, new particle formation or nucleation can create intermittent bursts in PNC. Nucleation is generally a regional phenomenon[43] and can vary seasonally. Therefore, the previously discussed seasonal correction factors should account for the effects of nucleation at any site with less than 1 year of data (Table S1). In addition, previous studies have shown that the contribution of freshly nucleated particles to the long-term average PNC at the urban background locations is relatively small (5−10%).[44,45]

2.3. Land-Use Regression Model Development. We combined the PNC data set (Figure 1) with a set of national land-use covariates (Table S2) to develop a land-use regression (LUR) model to predict annual average PNC for 2016−2017 at census blocks across the continental United States. Two things are critically important for LUR model development and predictions: (1) the measurement data used for model building should be representative of long-term average concentrations;[46] (2) the measurement locations used for model building should span the distribution of land-use covariates across the prediction domain.

The representativeness of our data set with respect to long-term averages and temporal corrections are discussed in Section 2.2. To assess the representativeness of our measurement locations, we compared the distribution of land-use covariates at our measurement locations to nationwide census blocks (Figures 1C and S6). The distribution of covariates at measurement locations spans the 0−99th percentile ranges of national distributions in all cases. This demonstrates the representativeness of sampling locations for developing a national model. Furthermore, when applying the model, we did not extrapolate it beyond the covariate values for the measurement locations used for model building (see Section 2.5).

Table S2 lists the covariates used for LUR model development. Land-use variables were compiled from various sources (e.g., NEI Database, TeleAtlas, US Census Bureau, USGS, National Landcover and elevation data, Bureau of Transportation); detailed information is available in Kim et al.[47] Variables include traffic, population, land-use type (commercial, transportation, industrial, residential, rural), surface imperviousness, latitude, longitude, elevation, restaurant count, distance from an airport, criteria pollutant emissions, and satellite air pollution estimates. Imperviousness refers to the percentage of area that is covered with an impervious surface, such as pavement or concrete. Each covariate was calculated for different buffer sizes from 100 m to 15 km at the centroid of each census block across the contiguous United States. Since our mobile PNC data from three cities were aggregated over a 1 km^2 grid, we averaged the covariate data over each grid cell and then assigned that value to the grid-cell center. For the fixed sites, we assigned the nearest census block's covariate data to the measurement location.

We used a stepwise forward selection regression method for the LUR model building, similar to the ESCAPE protocol.[36,39] The model selects variables one at a time, starting with the variable that provides the highest adjusted-R^2 (coefficient of determination) in univariate linear regressions. The variable selection process continues until a newly added variable improves the overall model R^2 by less than 0.01. Among the selected variables, we remove those with p values (predictor significance) greater than 0.05. Following the ESCAPE protocol, we also examined the Cook's D for influential observations, variance inflation factors (VIF) for collinearity, and Moran's I for spatial autocorrelation. We describe the model performance in terms of adjusted-R^2, root-mean-square error (RMSE), and normalized mean bias (NMB).

2.4. Model Evaluation. To characterize model performance, we performed three types of model evaluation: (i) traditional 10-fold cross-validation (CV) by randomly dividing the 118 measurement locations into 10 groups, (ii) defined spatial holdout cross-validation (similar to spatial clustered holdout[48]), and (iii) evaluation against a fully independent data set. For each evaluation, we computed performance statistics (R^2, RMSE, NMB) by comparing predicted versus measured concentrations at the holdout locations. We compared these statistics to the performance of the base model, developed by fitting the entire input data set.

For spatial clustered holdout, we remove specific subsets of the measurement data (e.g., all Oakland data), derive an LUR model using the remaining data, and then apply the model to predict concentrations at the holdout locations. This approach is a more stringent test than the traditional random CV[47,48] because it more rigorously tests the ability of the model to extrapolate in space. We performed seven spatial clustered holdouts. These include holding out the data from (i) Oakland, (ii) Pittsburgh, (iii) Baltimore, (iv) all other (fixed) urban sites, (v) near airport sites, (vi) half of the rural sites, and (vii) the other half of the rural sites. We performed rural holdout by randomly dividing all of the rural sites into two groups. We need to include some rural sites in each model to capture the rural background.

Finally, we evaluated model performance against a fully independent UFP data set from Pittsburgh. This data set is described in Saha et al.[16] It was collected by multiweek continuous PNC measurements in the winter of 2017 and 2018 at 30 fixed sites in Pittsburgh that span a wide range of urban land-use attributes. It is completely independent of the Pittsburgh mobile data set used for model development.

2.5. Predicted National Concentration Surface. We applied the LUR model to predict census block-level PNC across the contiguous United States. The census block is the smallest geographic unit used by the US Census Bureau (average population: 50, 5−95th percentile range: 2−174). In urban areas, blocks vary in size and shape but typically cover an area of ∼0.01 km^2. We only made predictions at census blocks with predictor variable values within the 1st and 99th percentile range of the measurement data set used for model development. This means that model predictions do not extrapolate in covariate space. After applying this constraint, the model predicts outdoor concentration at 6 056 703 residential census block centroids in the contiguous Unites States, which corresponds to 98.6% of the population. This constraint censors predictions for only 2% of census blocks (1.4% of the population) in the contiguous United States. Censored census blocks are generally in extremely urban (e.g.,

https://doi.org/10.1021/acs.est.1c03237
Environ. Sci. Technol. 2021, 55, 10320−10331

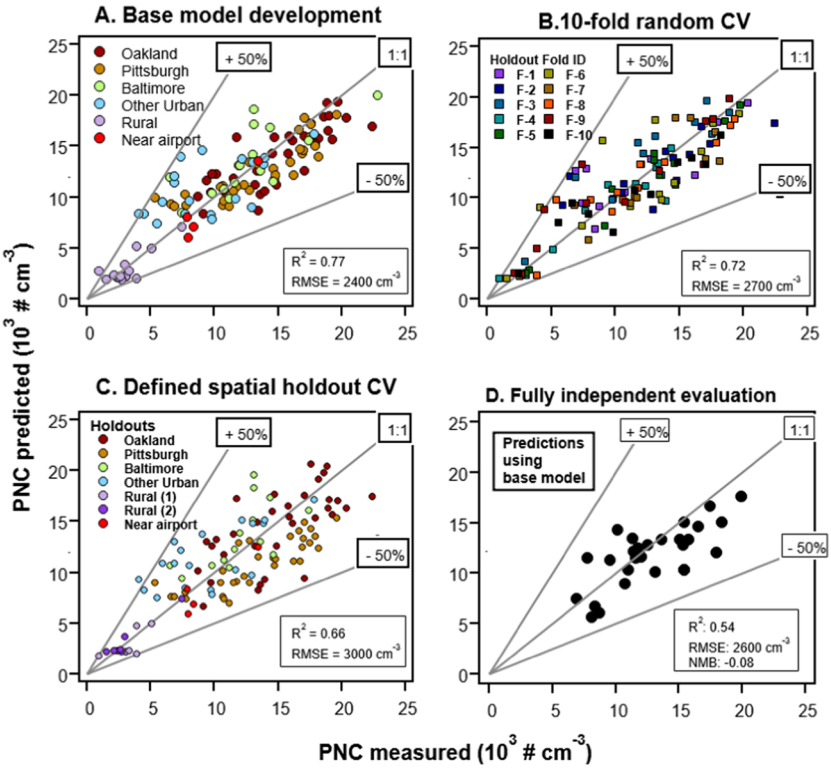

Figure 2. Model development and evaluation. (A) Base LUR model performance. (B) Random 10-folds cross-validation performance. (C) Spatially defined holdout cross-validation performance. (D) Independent evaluation of the base model against a 30-site stationary CPC network in Pittsburgh.

some blocks in Manhattan of New York City) and rural locations.

3. RESULTS

3.1. Spatial Variability in Measured Particle Number Concentrations. Figure 1 summarizes the PNC data used for LUR model development. The measured PNC ranges between ~1000 and 20 000 cm^{-3} with substantial variability between rural and urban, and within and between urban locations. The intraurban variability ranges from ~5000 to 20 000 cm^{-3}. The average urban PNC is ~3× larger than average rural PNC (rural: ~3000 cm^{-3}, urban: ~10 000 cm^{-3}). A large amount of variably exists within urban areas. For example, the mobile monitoring data show a factor of 3−4 in intracity PNC (ratio of 95th and 5th percentiles). In each mobile monitoring city (Figure 1), PNC is generally higher in downtown and commercial areas, indicating the importance of local sources that drive the intracity spatial variation of PNC in urban areas. The spatial variability in PNC is generally greater within- than between-city in the measured data set.

3.2. Land-Use Regression Model for Particle Number Concentration. Figure 2 summarizes the LUR development and evaluation results. Model parameters and performance metrics are listed in Table S3.

The base LUR model has an R^2 of 0.77 and RMSE of 2400 cm^{-3} (Figure 2A). The stepwise linear regression selected traffic and urbanicity covariates to explain the spatial variability in PNC. Specifically, the model uses five predictor variables: (i) impervious land surface within a 750 m buffer, (ii) inverse distance from the nearest highway, (iii) length of highway and city roads within a 3000 m buffer, (iv) commercial land-use area within a 1500 m buffer, and (v) residential land-use area within a 15 000 m buffer. The base LUR model has an intercept of 1800 cm^{-3}.

The selected variables are physically meaningful. For example, traffic is a known major source for PNC.[49] Commercial land-use and impervious surface are measures of urbanicity. PNC is higher in urban, commercial, and residential areas because of traffic and other urban sources like commercial and residential cooking. Many city-scale PNC LUR models identify similar land-use predictors.[50−64] There are likely other localized sources that are not accounted for in our model (as is true in any empirical LUR model).

Several recent field measurements indicate that aircraft operations can be an important source of ultrafine particles near very large airports.[31,65] Our model development included PNC data from four near airport sites. The distance from the nearest airport was included as a potential predictor variable. However, the stepwise regression did not select this parameter as a significant predictor variable. The impact of airports on ultrafine concentration is generally a localized phenomenon that depends on prevailing winds, flight volume, flight patterns, etc. It is not clear how airports will significantly impact PNC spatial patterns at the national level. Our defined holdout cross-validation (Figure 2C, discussed in Section 3.3) indicates that a model developed holding out all of the near airport data can reasonably predict PNC at these sites.

Our model R^2 is substantially better than most published city-scale PNC LUR models,[37,50−59,61−64] which generally have an R^2 of <0.5. Many city-scale models are derived from short-term stationary or mobile sampling with a limited amount of data (~1−3 days) per site. In comparison, our model is based on much longer time-averaged data. Since LUR modeling assumes representative mean concentrations,[46] the better

https://doi.org/10.1021/acs.est.1c03237
Environ. Sci. Technol. 2021, 55, 10320−10331

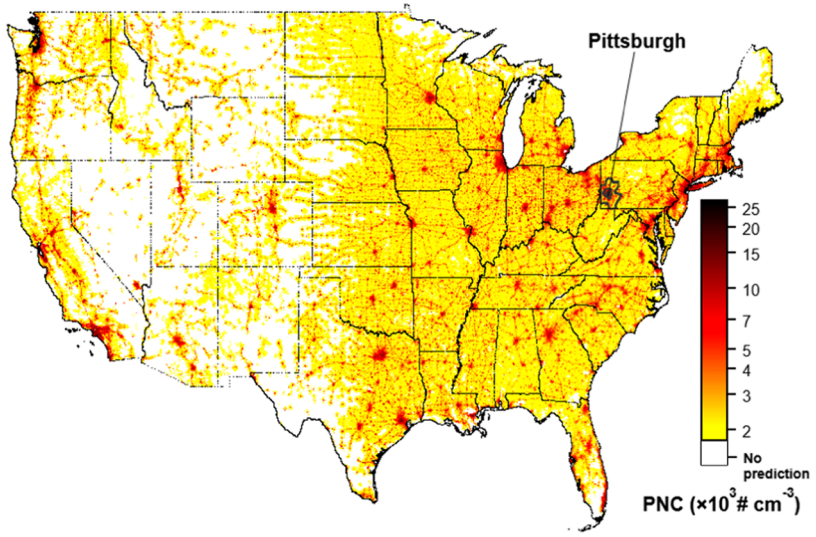

Figure 3. Census block PNC predictions across the contiguous United States. The color scale is in a log scale.

statistical performance of our model suggests that our data represent long-term average concentrations. A few city-scale models predict concentrations at finer temporal scales (e.g., hourly).[66] It is to be expected that the finer temporal resolution models might have lower R^2 compared to our annual average models.

3.3. Model Cross-Validation and Independent Evaluation. The three different distinct model-measurement evaluations (Figure 2B–D) yield a model performance R^2 of 0.54–0.72 and RMSE of 2600–3000 cm^{-3}. This level of performance is better than many published city-scale LUR models.[50−64]

First, conventional 10-fold cross-validation (CV) has an R^2 and RMSE of 0.72 and 2700 cm^{-3}, respectively (Figure 2B), which are similar to the base model (R^2 = 0.77; RMSE = 2400 cm^{-3}). In addition, independent variables selected by the stepwise regression for CV models (traffic and urbanicity related variables; see Table S3) are similar to the base model. This indicates that the model fit is not sensitive to random subsets of the data.

The spatial clustered holdout provides a more robust test of the ability to model to extrapolate in space. There are only modest differences between spatially clustered holdout CV (i.e., holdout data from individual cities, other urban or rural sites) (R^2 = 0.66, RMSE = 3000 cm^{-3}: Figure 2C) and the base model (R^2 = 0.77; RMSE = 2400 cm^{-3}). The stepwise regression selects similar independent variables for clustered CV models (Table S3) as for the base model. This indicates that the model provides robust extrapolations in space.

Finally, the model was evaluated against a fully independent data set (not used in any of the model building; Figure 2D) collected in Pittsburgh. This evaluation yields an R^2 = 0.54, RMSE = 2600 cm^{-3}, and normalized mean bias (NMB) = −8%. This level of performance against a completely independent data set is better than model building/cross-validation performance of many published city-scale LUR models.[50−64]

3.4. Predicted National Particle Number Concentration Surface. Figure 3 shows census block PNC predictions across the contiguous United States for 2016/2017. To our knowledge, this is the first high-spatial-resolution national PNC estimate in the United States. The predicted national census-block PNC range is between 1800 and 26 600 cm^{-3}. The national population-weighted PNC is ∼6500 cm^{-3}. This is lower than the typical urban PNC (∼10 000 cm^{-3}, Figure 1), but about 3 times the rural background (2000–3000 cm^{-3}). Predicted hotspots are in big cities and near highways.

Using census block predictions, we estimated the MSA (Metropolitan Statistical Area) and state-level population-weighted average PNC. An MSA usually consists of one big city (minimum population: 50 000) with multiple surrounding counties, townships, and suburban areas. MSA-average PNC vary between 3000 and 10 900 cm^{-3} (mean = 7700 cm^{-3}, n = 363); state-level average PNC vary between 3500 and 8600 cm^{-3} (mean = 5800 cm^{-3}, n = 48). PNC are higher in high-population-density areas of the mid-Atlantic, some parts of the Midwest, and in California. Thirteen states have PNC greater than the national average.

We compare our predicted national PNC surface with the national $PM_{2.5}$ and NO_2 estimates from Kim et al.[47] (see Figures S7 and S8). The spatial correlation between the national PNC and $PM_{2.5}$ surfaces is weak (R^2 values of 0.23 for nationwide census block-level concentrations; 0.03 for MSA-average concentrations; 0.05 for state-average concentrations; and 0.37 ± 0.20 for intracity (population > 100 000, n = 267)). The national PNC and NO_2 concentration surfaces are spatially correlated (R^2 values of 0.74 for nationwide census block-level concentrations; 0.64 for MSA-average; 0.76 for state-average; and 0.71 ± 0.15 for intracity (population > 100 000, n = 267)).

PNC and NO_2 are spatially correlated because traffic is an important source of both pollutants.[2] The moderate intracity PNC-$PM_{2.5}$ spatial correlation (e.g., average of 267 cities, R^2 = 0.37) is due to similar traffic and combustion-related sources driving intracity gradients of both pollutants.[26,27] However, as these urban emissions are transported over suburban and rural areas on a timescale of several days, the PNC reduces due to dispersion and coagulation and $PM_{2.5}$ mass increases due to secondary formation. This reduces the spatial correlation between PNC and $PM_{2.5}$ at the regional/national scale.

3.5. Intra- and Intercity Variations in Particle Number Concentrations. In this section, we use our predicted census-block-level PNC to investigate the intra- and intercity spatial patterns in PNC across the United States. First, to illustrate a

https://doi.org/10.1021/acs.est.1c03237
Environ. Sci. Technol. 2021, 55, 10320−10331

typical spatial pattern of PNC over a metro area, we show the data from Pittsburgh MSA as an example (Figure 4). Then, we examine data from all 267 US cities with a population > 100 000 to investigate the intra- and intercity spatial variations in PNC across the United States (Figure 5).

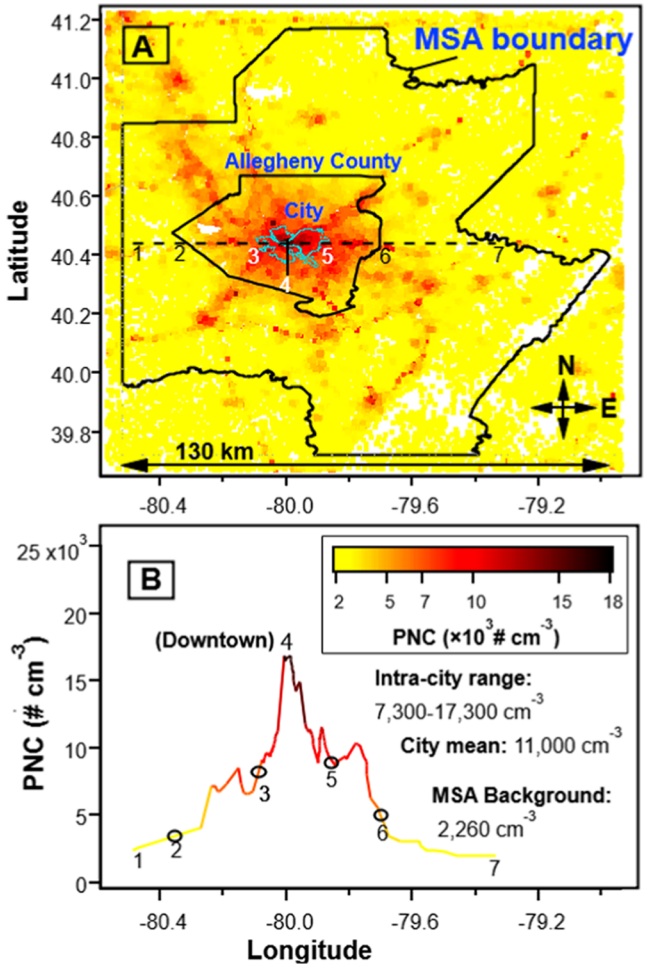

Figure 4. (A) Predicted PNC surface over Pittsburgh Metropolitan Statistical Area (MSA; FIPS Code 38300). (B) Transect profile that passes through the city center (downtown Pittsburgh) shows the distribution of PNC along the transect line (1−7). The color scale on panel (B) applies to both panels (A) and (B).

Figure 4A shows the zoom-in map of PNC over Pittsburgh MSA. Within the Pittsburgh MSA, PNC hotspots are in the city center and densely populated areas. The predicted PNC gradually decreases as one moves away from the city center (Figure 4B). For the Pittsburgh MSA, the background (defined as the fifth percentile of MSA-wide concentrations) PNC is 2260 cm^{-3}, the city-average PNC is 11 000 cm^{-3}, and the intracity range (1st−99th percentile) is 7300−17 300 cm^{-3}. Within the city of Pittsburgh, PNC varies by a factor of 2.5 (ratio of 99th and 1st percentile). The city background PNC is (7000−8000 cm^{-3}) about 2−4 times higher than the suburban and rural PNC in this MSA (2000−4000 cm^{-3}).

Figure 5 shows that these trends shown in Pittsburgh are consistent across the United States. It summarizes city average, MSA background, and intracity PNC for all 267 US cities with a population greater than 100 000. To provide context for results, we compare PNC with $PM_{2.5}$ mass concentrations in these cities. $PM_{2.5}$ data are annual average estimates in 2015 from Kim et al.[47] Again the PNC are annual average estimates in 2016−2017.

The city-average PNC varies between 5000 and 14 000 cm^{-3} across the 267 cities included in the analysis. This corresponds to a factor of 3 intercity variability. The city-average PNC is a factor of 2−4 higher than the MSA background levels (2000−4000 cm^{-3}). The city-average PNC is greater than 10 000 cm^{-3} in 63 cities, mostly big cities in California (CA: 25 cities), Northeast (NY: 5, NJ: 3, MA: 3, PA: 3), and Midwest.

Within a city, concentrations vary by a factor of 2−6 (ratio of 99th and 1st percentiles). The intracity variation is typically greater in a city with a larger land area (Figure S9). This is because a city with a larger land area likely has more dynamic land-use patterns (e.g., less-polluted suburban areas, more-polluted downtown/city center).

Compared to PNC, the intracity variations in $PM_{2.5}$ mass concentrations are substantially smaller, varying between 1.2 and 1.6 (ratio of 99th and 1st percentile). However, there are still large intercity variations in $PM_{2.5}$ mass (5−12 $\mu g\ m^{-3}$). The factor of 2.4 intercity variations in $PM_{2.5}$ mass is comparable to the intercity variations of PNC (a factor of 3).

While both PNC and $PM_{2.5}$ show a large intercity variation, the factors driving these patterns are likely different. For $PM_{2.5}$, intercity differences are likely due to secondary $PM_{2.5}$ formation. In the southeast, this is mainly (biogenic) secondary organic aerosol.[67] In the Midwest and northeast, it is primarily secondary inorganic aerosol (sulfate).[68] On the other hand, the predicted intercity variations in PNC are driven by primary sources (e.g., traffic, urbanicity, commercial, and residential land use). The city-average values of these predictor variables are higher in cities with higher city-average PNC, as expected (Figure S10).

3.6. Robustness of Predicted Particle Number Concentrations. A challenge for UFP exposure assessment is the lack of data. To overcome this limitation, we compiled measured PNC data from multiple sources. Potential consistency issues associated with combining data from different studies are discussed in Section 2.2. The national model is based on data from 118 locations. This raises concerns about whether there is enough data for building a national model and the representativeness and quality of these data. However, previous studies[36,38,46] demonstrate that the distribution of land-use covariates across the measurement locations is more important than the absolute number of sites. Beyond a certain number of locations that ensure spatial variability, additional sites with similar land-use variables may not add much additional value for LUR model development. The distributions of land-use covariates at our sampling locations basically span the entire range (0−99th percentile, at least) of the national covariate distribution (Figures 1C and S6). Therefore, our measurement locations provide a representative data set for national model development.

Our model explains about 77% of spatial variability of PNC concentrations measured at 118 locations using five predictor variables. Therefore, the model is not overfit. In addition, the model predictor variables are physically meaningful. Finally, there is strong model performance across different cross validations. In almost all cases, predicted PNC surfaces using various cross-validation (random 10-folds, defined spatial holdouts; Figure S11 and Table S3) and sensitivity analysis (models using a subset of 200 ×200 m^2 intracity data; Figure S12 and Table S4) agreed within 15% of the base model. This

https://doi.org/10.1021/acs.est.1c03237
Environ. Sci. Technol. 2021, 55, 10320−10331

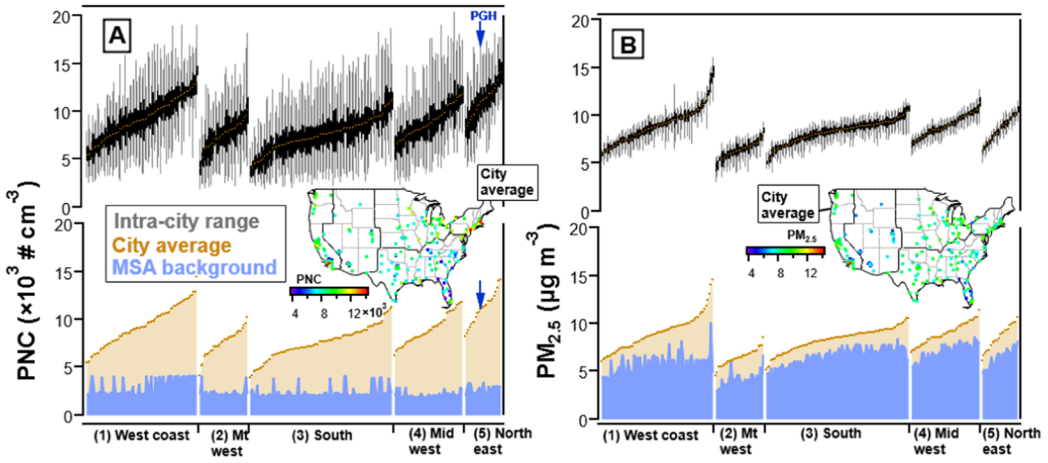

Figure 5. Intra- and intercity spatial variations of PNC and $PM_{2.5}$ in 267 US cities with a population > 100 000. Cities are grouped by region; within a region, cities are rank-ordered by city-average PNC (panel A) and $PM_{2.5}$ (panel B). (A, B: Lower): The MSA background (blue) is the fifth percentile of (census block-level) concentrations within an MSA boundary. City mean (orange dot) is the arithmetic mean of (census block level) concentrations within a city boundary. (A, B: middle): Maps show the spatial distribution of city-average concentrations. (A, B: Upper): Box-whisker plots show intracity variations in each city using census block-level concentrations within the city boundary (box (dark black): interquartile range, whisker: 1st and 99th percentile range, red dot: city mean). The location of Pittsburgh (for which analysis is shown in Figure 4) is marked by "PGH" on panel (A).

fact, combined with the relatively high quality of the model fit (see the Section 3.3), provides confidence that this data set and the resulting model provide a reasonable representation of long-term (~annual) average PNC.

Our predicted PNC variability (1800−26 000 cm^{-3}) is likely a conservative estimate of the actual spatial variability. This is a characteristic of LUR models, in general. Since we do not extrapolate in covariate space beyond the data set used for model building, we do not have predictions in some highly urbanized areas (e.g., extremely high-population-density areas in Manhattan). Concentrations in these areas may be larger than our predicted range. Our LUR model has an intercept of ~1800 cm^{-3}. Therefore, the predicted concentration in rural areas will always be greater than 1800 cm^{-3}. However, data from rural sites indicate PNC in remote areas can be as low as 1000 cm^{-3} (Figure 1). In general, our model overpredicts in some rural areas and underpredicts in high source areas (a typical limitation of any national LUR model).

4.0. DISCUSSION

Our model provides high-spatial-resolution (census block-level) national estimates of outdoor PNC. It predicts large urban−rural, intra-, and intercity contrasts in PNC. Our analysis indicates that PNC and $PM_{2.5}$ are moderately correlated at the city scales but uncorrelated at the regional and national scale. These high-spatial-resolution estimates are useful for population-based exposure analysis (e.g., socio-economic disparity analysis of air pollution exposure, epidemiological health impact analysis) and environmental policy analysis (e.g., spatial patterns and hotspots, air pollution regulation).

Due to the lack of large-spatial-scale exposure estimates, previous PNC epidemiological studies have only considered data from a single city or urbanized area.[10−12] The independent effects of PNC from $PM_{2.5}$ remain inconclusive in these studies. Since PNC and $PM_{2.5}$ are uncorrelated at the national scale, national-scale epidemiological studies may have more power to differentiate the independent effects of PNC from $PM_{2.5}$. Due to different spatial patterns, socioeconomic disparities to PNC versus $PM_{2.5}$ exposures are likely to be different.

Most large-scale population-based exposure studies are based on outdoor concentration estimates. Our model provides outdoor estimates of PNC. However, personal exposure can be different than outdoor concentrations. Exposure depends on where people spend time and varies between indoor and outdoor environments.[69−71] The indoor−outdoor contrast is much more critical for PNC than $PM_{2.5}$ mass concentrations.[72] Therefore, caution should be taken when interpreting exposure analysis results (e.g., epidemiological health analysis) applying outdoor concentration estimates.

The distinct spatial pattern of PNC versus $PM_{2.5}$ has implications for environmental policy and regulation. Current US regulations target $PM_{2.5}$ but not PNC. The intracity spatial distributions of PNC and $PM_{2.5}$ are very different, which suggests that regulation targeting sources of $PM_{2.5}$ mass may not reduce the PNC. For example, reducing secondary $PM_{2.5}$ is important for reducing $PM_{2.5}$ mass, but PNC is strongly related to traffic and urban sources. Therefore, regulations focused on traffic and urban air pollution sources are likely needed to reduce PNC.

Currently, a scarcity of monitoring data is a major challenge for national-scale ultrafine exposure assessment. The development of a high-spatial-density monitoring network over larger geographical areas is one solution for overcoming the data limitation. However, this strategy is complicated by the high cost of monitoring and the lack of regulatory requirements. Our results demonstrate that a hybrid monitoring approach that combines fixed sites and mobile data can be used to overcome the lack of routine monitoring data for the development of national-scale UFP concentration estimates.

Our model provides national estimates for a single point in time (2016−2017). However, time-series data are needed to allow for longitudinal exposure studies. Our results suggest that a hybrid long-term monitoring configuration could provide high-spatial-resolution concentration estimates in the United States. For example, such a network could include about 50

https://doi.org/10.1021/acs.est.1c03237
Environ. Sci. Technol. 2021, 55, 10320−10331

fixed sites at rural (20 sites) and urban (30 sites) background locations to capture the urban−rural and intercity variations and well-designed mobile sampling in three to five cities to capture the high-spatial-resolution intraurban spatial variability. Data at the selected locations need to be collected to characterize long-term (annual) average concentrations.

■ ASSOCIATED CONTENT

Supporting Information

The Supporting Information is available free of charge at https://pubs.acs.org/doi/10.1021/acs.est.1c03237.

Comparison of spatial averaging of mobile monitoring PNC data at 200 × 200 m^2 versus 1 km^2, trends in annual average PNC between 2006 and 2017 at a few urban and rural fixed sites, trends in monthly average PNC at a few urban and rural fixed sites, the measured particle size distributions data from a few urban and rural fixed sites, comparison of mobile monitoring and fixed-site PNC data from Pittsburgh, comparison of the distribution of land-use covariates at measurement locations and nationwide census blocks, comparison of predicted national PNC surface with the national $PM_{2.5}$ and NO_2 estimates, spatial correlation between PNC and $PM_{2.5}/NO_2$, correlation between intracity variations in PNC and city land area, relationship between city-average PNC and city-average land-use variables, comparison of the base model predictions with different holdout cross-validation models, comparison of the predicted national PNC surfaces with 1 km^2 versus 200 × 200 m^2 spatial averaging of mobile monitoring data, description of the PNC data used for LUR model development, description of land-use covariates used for PNC LUR model development, list of PNC LUR models parameters and performances, and list of parameters and performances of the PNC LUR models developed using a subset of 200 × 200 m^2 spatial averaging mobile data (PDF)

■ AUTHOR INFORMATION

Corresponding Authors

Allen L. Robinson − *Center for Atmospheric Particle Studies, Carnegie Mellon University, Pittsburgh, Pennsylvania 15213, United States; Department of Mechanical Engineering, Carnegie Mellon University, Pittsburgh, Pennsylvania 15213, United States;* orcid.org/0000-0002-1819-083X; Phone: 412-721-5203; Email: alr@andrew.cmu.edu; Fax: 412-268-3657

Albert A. Presto − *Center for Atmospheric Particle Studies, Carnegie Mellon University, Pittsburgh, Pennsylvania 15213, United States; Department of Mechanical Engineering, Carnegie Mellon University, Pittsburgh, Pennsylvania 15213, United States;* orcid.org/0000-0002-9156-1094; Email: apresto@andrew.cmu.edu

Authors

Provat K. Saha − *Center for Atmospheric Particle Studies, Carnegie Mellon University, Pittsburgh, Pennsylvania 15213, United States; Department of Mechanical Engineering, Carnegie Mellon University, Pittsburgh, Pennsylvania 15213, United States;* orcid.org/0000-0002-4044-9350

Steve Hankey − *School of Public and International Affairs, Virginia Tech, Blacksburg, Virginia 24061, United States;* orcid.org/0000-0002-7530-6077

Julian D. Marshall − *Department of Civil and Environmental Engineering, University of Washington, Seattle, Washington 98195, United States;* orcid.org/0000-0003-4087-1209

Complete contact information is available at: https://pubs.acs.org/10.1021/acs.est.1c03237

Notes

The authors declare no competing financial interest.

Predicted census-block-level PNC in the contiguous United States is publicly and freely available online at (https://www.caces.us).

■ ACKNOWLEDGMENTS

This research was conducted as part of the Center for Air, Climate, and Energy Solutions (CACES), which was supported by the Environmental Protection Agency (assistance agreement number RD83587301). It has not been formally reviewed by EPA. The views expressed in this document are solely those of authors and do not necessarily reflect those of the Agency. EPA does not endorse any products or commercial services mentioned in this publication.

■ REFERENCES

(1) Cohen, A. J.; Brauer, M.; Burnett, R.; Anderson, H. R.; Frostad, J.; Estep, K.; Balakrishnan, K.; Brunekreef, B.; Dandona, L.; Dandona, R.; Feigin, V.; Freedman, G.; Hubbell, B.; Jobling, A.; Kan, H.; Knibbs, L.; Liu, Y.; Martin, R.; Morawska, L.; Pope, C. A.; Shin, H.; Straif, K.; Shaddick, G.; Thomas, M.; van Dingenen, R.; van Donkelaar, A.; Vos, T.; Murray, C. J. L.; Forouzanfar, M. H. Estimates and 25-Year Trends of the Global Burden of Disease Attributable to Ambient Air Pollution: An Analysis of Data from the Global Burden of Diseases Study 2015. *Lancet* **2017**, *389*, 1907−1918.

(2) HEI. *Understanding the Health Effects of Ambient Ultrafine Particles*; HEI Perspectives 3; Health Effects Institute: Boston, MA, 2013.

(3) Chen, R.; Hu, B.; Liu, Y.; Xu, J.; Yang, G.; Xu, D.; Chen, C. Beyond PM2.5: The Role of Ultrafine Particles on Adverse Health Effects of Air Pollution. *Biochim. Biophys. Acta, Gen. Subj.* **2016**, *1860*, 2844−2855.

(4) Oberdorster, G. Toxicology of Ultrafine Particles: In Vivo Studies. *Philos. Trans. R. Soc., A* **2000**, *358*, 2719−2740.

(5) Delfino, R. J.; Sioutas, C.; Malik, S. Potential Role of Ultrafine Particles in Associations between Airborne Particle Mass and Cardiovascular Health. *Environ. Health Perspect.* **2005**, *113*, 934−946.

(6) Baldauf, R. W.; Devlin, R. B.; Gehr, P.; Giannelli, R.; Hassett-Sipple, B.; Jung, H.; Martini, G.; McDonald, J.; Sacks, J. D.; Walker, K. Ultrafine Particle Metrics and Research Considerations: Review of the 2015 UFP Workshop. *Int. J. Environ. Res. Public Health* **2016**, *13*, No. 1054.

(7) Li, N.; Sioutas, C.; Cho, A.; Schmitz, D.; Misra, C.; Sempf, J.; Wang, M.; Oberley, T.; Froines, J.; Nel, A. Ultrafine Particulate Pollutants Induce Oxidative Stress and Mitochondrial Damage. *Environ. Health Perspect.* **2003**, *111*, 455−460.

(8) Schmid, O.; Möller, W.; Semmler-Behnke, M.; Ferron, G. A.; Karg, E.; Lipka, J.; Schulz, H.; Kreyling, W. G.; Stoeger, T. Dosimetry and Toxicology of Inhaled Ultrafine Particles. *Biomarkers* **2009**, *14*, 67−73.

(9) Andersen, Z. J.; Olsen, T. S.; Andersen, K. K.; Loft, S.; Ketzel, M.; Raaschou-Nielsen, O. Association between Short-Term Exposure to Ultrafine Particles and Hospital Admissions for Stroke in Copenhagen, Denmark. *Eur. Heart J.* **2010**, *31*, 2034−2040.

(10) Downward, G. S.; van Nunen, E. J. H. M.; Kerckhoffs, J.; Vineis, P.; Brunekreef, B.; Boer, J. M. A.; Messier, K. P.; Roy, A.; Verschuren, W. M. M.; van der Schouw, Y. T.; Sluijs, I.; Gulliver, J.; Hoek, G.; Vermeulen, R. Long-Term Exposure to Ultrafine Particles and Incidence of Cardiovascular and Cerebrovascular Disease in a Prospective Study of a Dutch Cohort. *Environ. Health Perspect.* **2018**, *126*, No. 127007.
(11) Weichenthal, S.; Bai, L.; Hatzopoulou, M.; Van Ryswyk, K.; Kwong, J. C.; Jerrett, M.; van Donkelaar, A.; Martin, R. V.; Burnett, R. T.; Lu, H.; Chen, H. Long-Term Exposure to Ambient Ultrafine Particles and Respiratory Disease Incidence in in Toronto, Canada: A Cohort Study. *Environ. Health* **2017**, *16*, No. 64.
(12) Ostro, B.; Hu, J.; Goldberg, D.; Reynolds, P.; Hertz, A.; Bernstein, L.; Kleeman, M. J. Associations of Mortality with Long-Term Exposures to Fine and Ultrafine Particles, Species and Sources: Results from the California Teachers Study Cohort. *Environ. Health Perspect.* **2015**, *123*, 549−556.
(13) Ohlwein, S.; Kappeler, R.; Kutlar Joss, M.; Künzli, N.; Hoffmann, B. Health Effects of Ultrafine Particles: A Systematic Literature Review Update of Epidemiological Evidence. *Int. J. Public Health* **2019**, *64*, 547−559.
(14) Sioutas, C.; Delfino, R. J.; Singh, M. Exposure Assessment for Atmospheric Ultrafine Particles (UFPs) and Implications in Epidemiologic Research. *Environ. Health Perspect.* **2005**, *113*, 947−955.
(15) Pekkanen, J.; Kulmala, M. Exposure Assessment of Ultrafine Particles in Epidemiologic Time-Series Studies. *Scand. J. Work, Environ. Health* **2004**, *30*, 9−18.
(16) Saha, P. K.; Zimmerman, N.; Malings, C.; Hauryliuk, A.; Li, Z.; Snell, L.; Subramanian, R.; Lipsky, E.; Apte, J. S.; Robinson, A. L.; Presto, A. A. Quantifying High-Resolution Spatial Variations and Local Source Impacts of Urban Ultrafine Particle Concentrations. *Sci. Total Environ.* **2019**, *655*, 473−481.
(17) Kumar, P.; Robins, A.; Vardoulakis, S.; Britter, R. A Review of the Characteristics of Nanoparticles in the Urban Atmosphere and the Prospects for Developing Regulatory Controls. *Atmos. Environ.* **2010**, *44*, 5035−5052.
(18) Hankey, S.; Marshall, J. D. On-Bicycle Exposure to Particulate Air Pollution: Particle Number, Black Carbon, PM2.5, and Particle Size. *Atmos. Environ.* **2015**, *122*, 65−73.
(19) Eeftens, M.; Phuleria, H. C.; Meier, R.; Aguilera, I.; Corradi, E.; Davey, M.; Ducret-Stich, R.; Fierz, M.; Gehrig, R.; Ineichen, A.; Keidel, D.; Probst-Hensch, N.; Ragettli, M. S.; Schindler, C.; Künzli, N.; Tsai, M.-Y. Spatial and Temporal Variability of Ultrafine Particles, NO2, PM2.5, PM2.5 Absorbance, PM10 and PMcoarse in Swiss Study Areas. *Atmos. Environ.* **2015**, *111*, 60−70.
(20) Wang, Y.; Hopke, P. K.; Utell, M. J. Urban-Scale Seasonal and Spatial Variability of Ultrafine Particle Number Concentrations. *Water Air Soil Pollut.* **2012**, *223*, 2223−2235.
(21) Demerjian, K. L. A Review of National Monitoring Networks in North America. *Atmos. Environ.* **2000**, *34*, 1861−1884.
(22) Apte, J. S.; Messier, K. P.; Gani, S.; Brauer, M.; Kirchstetter, T. W.; Lunden, M. M.; Marshall, J. D.; Portier, C. J.; Vermeulen, R. C. H.; Hamburg, S. P. High-Resolution Air Pollution Mapping with Google Street View Cars: Exploiting Big Data. *Environ. Sci. Technol.* **2017**, *51*, 6999−7008.
(23) Wilson, J. G.; Kingham, S.; Pearce, J.; Sturman, A. P. A Review of Intraurban Variations in Particulate Air Pollution: Implications for Epidemiological Research. *Atmos. Environ.* **2005**, *39*, 6444−6462.
(24) Li, H. Z.; Gu, P.; Ye, Q.; Zimmerman, N.; Robinson, E. S.; Subramanian, R.; Apte, J. S.; Robinson, A. L.; Presto, A. A. Spatially Dense Air Pollutant Sampling: Implications of Spatial Variability on the Representativeness of Stationary Air Pollutant Monitors. *Atmos. Environ. X* **2019**, *2*, No. 100012.
(25) Özkaynak, H.; Baxter, L. K.; Dionisio, K. L.; Burke, J. Air Pollution Exposure Prediction Approaches Used in Air Pollution Epidemiology Studies. *J. Exposure Sci. Environ. Epidemiol.* **2013**, *23*, 566−572.
(26) Saha, P. K.; Sengupta, S.; Adams, P.; Robinson, A. L.; Presto, A. A. Spatial Correlation of Ultrafine Particle Number and Fine Particle Mass at Urban Scales: Implications for Health Assessment. *Environ. Sci. Technol.* **2020**, *54*, 9295−9304.
(27) Levy, I.; Mihele, C.; Lu, G.; Narayan, J.; Brook, J. R. Evaluating Multipollutant Exposure and Urban Air Quality: Pollutant Interrelationships, Neighborhood Variability, and Nitrogen Dioxide as a Proxy Pollutant. *Environ. Health Perspect.* **2014**, *122*, 65−72.
(28) Krall, J. R.; Chang, H. H.; Sarnat, S. E.; Peng, R. D.; Waller, L. A. Current Methods and Challenges for Epidemiological Studies of the Associations Between Chemical Constituents of Particulate Matter and Health. *Curr. Environ. Health Rep.* **2015**, *2*, 388−398.
(29) Presto, A. A.; Saha, P. K.; Robinson, A. L. Past, Present, and Future of Ultrafine Particle Exposures in North America. *Atmos. Environ. X* **2021**, *10*, No. 100109.
(30) Hudda, N.; Simon, M. C.; Zamore, W.; Durant, J. L. Aviation-Related Impacts on Ultrafine Particle Number Concentrations Outside and Inside Residences near an Airport. *Environ. Sci. Technol.* **2018**, *52*, 1765−1772.
(31) Hudda, N.; Gould, T.; Hartin, K.; Larson, T. V.; Fruin, S. A. Emissions from an International Airport Increase Particle Number Concentrations 4-Fold at 10 Km Downwind. *Environ. Sci. Technol.* **2014**, *48*, 6628−6635.
(32) Austin, E.; Xiang, J.; Gould, T. R.; Shirai, J. H.; Yun, S.; Yost, M. G.; Larson, T. V.; Seto, E. Distinct Ultrafine Particle Profiles Associated with Aircraft and Roadway Traffic. *Environ. Sci. Technol.* **2021**, *55*, 2847−2858.
(33) Hering, S. V.; Spielman, S. R.; Lewis, G. S. Moderated, Water-Based, Condensational Particle Growth in a Laminar Flow. *Aerosol Sci. Technol.* **2014**, *48*, 401−408.
(34) Shah, R. U.; Robinson, E. S.; Gu, P.; Robinson, A. L.; Apte, J. S.; Presto, A. A. High-Spatial-Resolution Mapping and Source Apportionment of Aerosol Composition in Oakland, California, Using Mobile Aerosol Mass Spectrometry. *Atmos. Chem. Phys.* **2018**, *18*, 16325−16344.
(35) Robinson, E. S.; Gu, P.; Ye, Q.; Li, H. Z.; Shah, R. U.; Apte, J. S.; Robinson, A. L.; Presto, A. A. Restaurant Impacts on Outdoor Air Quality: Elevated Organic Aerosol Mass from Restaurant Cooking with Neighborhood-Scale Plume Extents. *Environ. Sci. Technol.* **2018**, *52*, 9285−9294.
(36) Saha, P. K.; Li, H. Z.; Apte, J. S.; Robinson, A. L.; Presto, A. A. Urban Ultrafine Particle Exposure Assessment with Land-Use Regression: Influence of Sampling Strategy. *Environ. Sci. Technol.* **2019**, *53*, 7326−7336.
(37) Messier, K. P.; Chambliss, S. E.; Gani, S.; Alvarez, R.; Brauer, M.; Choi, J. J.; Hamburg, S. P.; Kerckhoffs, J.; LaFranchi, B.; Lunden, M. M.; Marshall, J. D.; Portier, C. J.; Roy, A.; Szpiro, A. A.; Vermeulen, R. C. H.; Apte, J. S. Mapping Air Pollution with Google Street View Cars: Efficient Approaches with Mobile Monitoring and Land Use Regression. *Environ. Sci. Technol.* **2018**, *52*, 12563−12572.
(38) Hatzopoulou, M.; Valois, M. F.; Levy, I.; Mihele, C.; Lu, G.; Bagg, S.; Minet, L.; Brook, J. Robustness of Land-Use Regression Models Developed from Mobile Air Pollutant Measurements. *Environ. Sci. Technol.* **2017**, *51*, 3938−3947.
(39) Eeftens, M.; Beelen, R.; de Hoogh, K.; Bellander, T.; Cesaroni, G.; Cirach, M.; Declercq, C.; Dėdelė, A.; Dons, E.; de Nazelle, A.; Dimakopoulou, K.; Eriksen, K.; Falq, G.; Fischer, P.; Galassi, C.; Gražulevičienė, R.; Heinrich, J.; Hoffmann, B.; Jerrett, M.; Keidel, D.; Korek, M.; Lanki, T.; Lindley, S.; Madsen, C.; Mölter, A.; Nádor, G.; Nieuwenhuijsen, M.; Nonnemacher, M.; Pedeli, X.; Raaschou-Nielsen, O.; Patelarou, E.; Quass, U.; Ranzi, A.; Schindler, C.; Stempfelet, M.; Stephanou, E.; Sugiri, D.; Tsai, M.-Y.; Yli-Tuomi, T.; Varró, M. J.; Vienneau, D.; Klot, S.; von Wolf, K.; Brunekreef, B.; Hoek, G. Development of Land Use Regression Models for PM2.5, PM2.5 Absorbance, PM10 and PMcoarse in 20 European Study Areas; Results of the ESCAPE Project. *Environ. Sci. Technol.* **2012**, *46*, 11195−11205.
(40) Beelen, R.; Hoek, G.; Vienneau, D.; Eeftens, M.; Dimakopoulou, K.; Pedeli, X.; Tsai, M.-Y.; Künzli, N.; Schikowski,

https://doi.org/10.1021/acs.est.1c03237
Environ. Sci. Technol. 2021, 55, 10320−10331

T.; Marcon, A.; Eriksen, K. T.; Raaschou-Nielsen, O.; Stephanou, E.; Patelarou, E.; Lanki, T.; Yli-Tuomi, T.; Declercq, C.; Falq, G.; Stempfelet, M.; Birk, M.; Cyrys, J.; von Klot, S.; Nádor, G.; Varró, M. J.; Dėdelė, A.; Gražulevičienė, R.; Mölter, A.; Lindley, S.; Madsen, C.; Cesaroni, G.; Ranzi, A.; Badaloni, C.; Hoffmann, B.; Nonnemacher, M.; Krämer, U.; Kuhlbusch, T.; Cirach, M.; de Nazelle, A.; Nieuwenhuijsen, M.; Bellander, T.; Korek, M.; Olsson, D.; Strömgren, M.; Dons, E.; Jerrett, M.; Fischer, P.; Wang, M.; Brunekreef, B.; de Hoogh, K. Development of NO2 and NOx Land Use Regression Models for Estimating Air Pollution Exposure in 36 Study Areas in Europe—The ESCAPE Project. *Atmos. Environ.* **2013**, *72*, 10−23.

(41) Kerckhoffs, J.; Hoek, G.; Messier, K. P.; Brunekreef, B.; Meliefste, K.; Klompmaker, J. O.; Vermeulen, R. Comparison of Ultrafine Particle and Black Carbon Concentration Predictions from a Mobile and Short-Term Stationary Land-Use Regression Model. *Environ. Sci. Technol.* **2016**, *50*, 12894−12902.

(42) Minet, L.; Liu, R.; Valois, M.-F.; Xu, J.; Weichenthal, S.; Hatzopoulou, M. Development and Comparison of Air Pollution Exposure Surfaces Derived from On-Road Mobile Monitoring and Short-Term Stationary Sidewalk Measurements. *Environ. Sci. Technol.* **2018**, *52*, 3512−3519.

(43) Kulmala, M.; Maso, M. D.; Mäkelä, J. M.; Pirjola, L.; Väkevä, M.; Aalto, P.; Miikkulainen, P.; Hämeri, K.; O'dowd, C. D. On the Formation, Growth and Composition of Nucleation Mode Particles. *Tellus B* **2001**, *53*, 479−490.

(44) Saha, P. K.; Robinson, E. S.; Shah, R. U.; Zimmerman, N.; Apte, J. S.; Robinson, A. L.; Presto, A. A. Reduced Ultrafine Particle Concentration in Urban Air: Changes in Nucleation and Anthropogenic Emissions. *Environ. Sci. Technol.* **2018**, *52*, 6798−6806.

(45) Brines, M.; Dall'Osto, M.; Beddows, D. C. S.; Harrison, R. M.; Gómez-Moreno, F.; Núñez, L.; Artíñano, B.; Costabile, F.; Gobbi, G. P.; Salimi, F.; Morawska, L.; Sioutas, C.; Querol, X. Traffic and Nucleation Events as Main Sources of Ultrafine Particles in High-Insolation Developed World Cities. *Atmos. Chem. Phys.* **2015**, *15*, 5929−5945.

(46) Hoek, G. Methods for Assessing Long-Term Exposures to Outdoor Air Pollutants. *Curr. Environ. Health Rep.* **2017**, *4*, 450−462.

(47) Kim, S.-Y.; Bechle, M.; Hankey, S.; Sheppard, L.; Szpiro, A. A.; Marshall, J. D. Concentrations of Criteria Pollutants in the Contiguous U.S., 1979−2015: Role of Prediction Model Parsimony in Integrated Empirical Geographic Regression. *PLoS One* **2020**, *15*, No. e0228535.

(48) Young, M. T.; Bechle, M. J.; Sampson, P. D.; Szpiro, A. A.; Marshall, J. D.; Sheppard, L.; Kaufman, J. D. Satellite-Based NO2 and Model Validation in a National Prediction Model Based on Universal Kriging and Land-Use Regression. *Environ. Sci. Technol.* **2016**, *50*, 3686−3694.

(49) Kumar, P.; Morawska, L.; Birmili, W.; Paasonen, P.; Hu, M.; Kulmala, M.; Harrison, R. M.; Norford, L.; Britter, R. Ultrafine Particles in Cities. *Environ. Int.* **2014**, *66*, 1−10.

(50) Minet, L.; Liu, R.; Valois, M.-F.; Xu, J.; Weichenthal, S.; Hatzopoulou, M. Development and Comparison of Air Pollution Exposure Surfaces Derived from On-Road Mobile Monitoring and Short-Term Stationary Sidewalk Measurements. *Environ. Sci. Technol.* **2018**, *52*, 3512−3519.

(51) Hankey, S.; Marshall, J. D. Land Use Regression Models of On-Road Particulate Air Pollution (Particle Number, Black Carbon, PM2.5, Particle Size) Using Mobile Monitoring. *Environ. Sci. Technol.* **2015**, *49*, 9194−9202.

(52) Kerckhoffs, J.; Hoek, G.; Messier, K. P.; Brunekreef, B.; Meliefste, K.; Klompmaker, J. O.; Vermeulen, R. Comparison of Ultrafine Particle and Black Carbon Concentration Predictions from a Mobile and Short-Term Stationary Land-Use Regression Model. *Environ. Sci. Technol.* **2016**, *50*, 12894−12902.

(53) Patton, A. P.; Zamore, W.; Naumova, E. N.; Levy, J. I.; Brugge, D.; Durant, J. L. Transferability and Generalizability of Regression Models of Ultrafine Particles in Urban Neighborhoods in the Boston Area. *Environ. Sci. Technol.* **2015**, *49*, 6051−6060.

(54) Abernethy, R. C.; Allen, R. W.; McKendry, I. G.; Brauer, M. A Land Use Regression Model for Ultrafine Particles in Vancouver, Canada. *Environ. Sci. Technol.* **2013**, *47*, 5217−5225.

(55) Montagne, D. R.; Hoek, G.; Klompmaker, J. O.; Wang, M.; Meliefste, K.; Brunekreef, B. Land Use Regression Models for Ultrafine Particles and Black Carbon Based on Short-Term Monitoring Predict Past Spatial Variation. *Environ. Sci. Technol.* **2015**, *49*, 8712−8720.

(56) van Nunen, E.; Vermeulen, R.; Tsai, M.-Y.; Probst-Hensch, N.; Ineichen, A.; Davey, M.; Imboden, M.; Ducret-Stich, R.; Naccarati, A.; Raffaele, D.; Ranzi, A.; Ivaldi, C.; Galassi, C.; Nieuwenhuijsen, M.; Curto, A.; Donaire-Gonzalez, D.; Cirach, M.; Chatzi, L.; Kampouri, M.; Vlaanderen, J.; Meliefste, K.; Buijtenhuijs, D.; Brunekreef, B.; Morley, D.; Vineis, P.; Gulliver, J.; Hoek, G. Land Use Regression Models for Ultrafine Particles in Six European Areas. *Environ. Sci. Technol.* **2017**, *51*, 3336−3345.

(57) Ragettli, M. S.; Ducret-Stich, R. E.; Foraster, M.; Morelli, X.; Aguilera, I.; Basagaña, X.; Corradi, E.; Ineichen, A.; Tsai, M.-Y.; Probst-Hensch, N.; Rivera, M.; Slama, R.; Künzli, N.; Phuleria, H. C. Spatio-Temporal Variation of Urban Ultrafine Particle Number Concentrations. *Atmos. Environ.* **2014**, *96*, 275−283.

(58) Saraswat, A.; Apte, J. S.; Kandlikar, M.; Brauer, M.; Henderson, S. B.; Marshall, J. D. Spatiotemporal Land Use Regression Models of Fine, Ultrafine, and Black Carbon Particulate Matter in New Delhi, India. *Environ. Sci. Technol.* **2013**, *47*, 12903−12911.

(59) Weichenthal, S.; Ryswyk, K. V.; Goldstein, A.; Bagg, S.; Shekkarizfard, M.; Hatzopoulou, M. A Land Use Regression Model for Ambient Ultrafine Particles in Montreal, Canada: A Comparison of Linear Regression and a Machine Learning Approach. *Environ. Res.* **2016**, *146*, 65−72.

(60) Messier, K. P.; Chambliss, S. E.; Gani, S.; Alvarez, R.; Brauer, M.; Choi, J. J.; Hamburg, S. P.; Kerckhoffs, J.; LaFranchi, B.; Lunden, M. M.; Marshall, J. D.; Portier, C. J.; Roy, A.; Szpiro, A. A.; Vermeulen, R. C. H.; Apte, J. S. Mapping Air Pollution with Google Street View Cars: Efficient Approaches with Mobile Monitoring and Land Use Regression. *Environ. Sci. Technol.* **2018**, *52*, 12563−12572.

(61) Sabaliauskas, K.; Jeong, C.-H.; Yao, X.; Reali, C.; Sun, T.; Evans, G. J. Development of a Land-Use Regression Model for Ultrafine Particles in Toronto, Canada. *Atmos. Environ.* **2015**, *110*, 84−92.

(62) Farrell, W.; Weichenthal, S.; Goldberg, M.; Valois, M.-F.; Shekarrizfard, M.; Hatzopoulou, M. Near Roadway Air Pollution across a Spatially Extensive Road and Cycling Network. *Environ. Pollut.* **2016**, *212*, 498−507.

(63) Rivera, M.; Basagaña, X.; Aguilera, I.; Agis, D.; Bouso, L.; Foraster, M.; Medina-Ramón, M.; Pey, J.; Künzli, N.; Hoek, G. Spatial Distribution of Ultrafine Particles in Urban Settings: A Land Use Regression Model. *Atmos. Environ.* **2012**, *54*, 657−666.

(64) Simon, M. C.; Patton, A. P.; Naumova, E. N.; Levy, J. I.; Kumar, P.; Brugge, D.; Durant, J. L. Combining Measurements from Mobile Monitoring and a Reference Site To Develop Models of Ambient Ultrafine Particle Number Concentration at Residences. *Environ. Sci. Technol.* **2018**, *52*, 6985−6995.

(65) Pirhadi, M.; Mousavi, A.; Sowlat, M. H.; Janssen, N. A. H.; Cassee, F. R.; Sioutas, C. Relative Contributions of a Major International Airport Activities and Other Urban Sources to the Particle Number Concentrations (PNCs) at a Nearby Monitoring Site. *Environ. Pollut.* **2020**, *260*, No. 114027.

(66) Patton, A. P.; Collins, C.; Naumova, E. N.; Zamore, W.; Brugge, D.; Durant, J. L. An Hourly Regression Model for Ultrafine Particles in a Near-Highway Urban Area. *Environ. Sci. Technol.* **2014**, *48*, 3272−3280.

(67) Goldstein, A. H.; Koven, C. D.; Heald, C. L.; Fung, I. Y. Biogenic Carbon and Anthropogenic Pollutants Combine to Form a Cooling Haze over the Southeastern United States. *Proc. Natl. Acad. Sci. U.S.A.* **2009**, *106*, 8835−8840.

(68) Yang, Y.; Wang, H.; Smith, S. J.; Zhang, R.; Lou, S.; Yu, H.; Li, C.; Rasch, P. J. Source Apportionments of Aerosols and Their Direct

https://doi.org/10.1021/acs.est.1c03237
Environ. Sci. Technol. 2021, 55, 10320−10331

Radiative Forcing and Long-Term Trends Over Continental United States. *Earths Future* **2018**, *6*, 793−808.
(69) Meier, R.; Eeftens, M.; Phuleria, H. C.; Ineichen, A.; Corradi, E.; Davey, M.; Fierz, M.; Ducret-Stich, R. E.; Aguilera, I.; Schindler, C.; Rochat, T.; Probst-Hensch, N.; Tsai, M.-Y.; Künzli, N. Differences in Indoor versus Outdoor Concentrations of Ultrafine Particles, PM 2.5, PM Absorbance and NO 2 in Swiss Homes. *J. Exposure Sci. Environ. Epidemiol.* **2015**, *25*, 499−505.
(70) Wallace, L.; Ott, W. Personal Exposure to Ultrafine Particles. *J. Exposure Sci. Environ. Epidemiol.* **2011**, *21*, 20−30.
(71) Cattaneo, A.; Garramone, G.; Taronna, M.; Peruzzo, C.; Cavallo, D. M. Personal Exposure to Airborne Ultrafine Particles in the Urban Area of Milan. *J. Phys. Conf. Ser.* **2009**, *151*, No. 012039.
(72) Chen, C.; Zhao, B. Review of Relationship between Indoor and Outdoor Particles: I/O Ratio, Infiltration Factor and Penetration Factor. *Atmos. Environ.* **2011**, *45*, 275−288.

https://doi.org/10.1021/acs.est.1c03237
Environ. Sci. Technol. 2021, 55, 10320−10331